

## Toolpath generation method for four-axis NC machining of helical rotor

J.N. Lee\*, C.B. Huang, T.C. Chen

Division of, Department of Mechanical Engineering, Cheng Shiu University  
No. 840, Cheng-Ching RD., Niasong Township City, Kaohsiung County, 833, Taiwan

\* Corresponding author: E-mail address: jengnan@csu.edu.tw

Received 11.09.2008; published in revised form 01.12.2008

### Analysis and modelling

#### ABSTRACT

**Purpose:** This paper presented a method for generating the toolpaths for the machining of a helical rotor on five-axis machine tool.

**Design/methodology/approach:** The geometry of the helical rotor is designed based on the ruled surfaces. Through the homogeneous coordinate transformation, the cutter location of the flank milling for four-axis machining can be generated. The postprocessor are developed for converting the cutter location file to the four-axis numerical control program.

**Findings:** The toolpath generated are verified through solid cutting simulation and a trial cut. The results show that the proposed method is valid and the machining process works well.

**Practical implications:** As a result, modeling based on ruled surface is frequently used in constructing curved surfaces for aerospace industry and precision mechanical parts such as spatial cams, turbines, dies and molds, rotors of pumps, and centrifugal impellers.

**Originality/value:** This paper describes multi – axis toolpath generation using the flank milling method for the helical rotor, the cutter location file can be generated with cylindrical and mill.

**Keywords:** Helical rotor; Ruled surface; Four-axis machining; Toolpath; Postprocessor

### 1. Introduction

A ruled surface is generated by a straight line (also called rulings or generators) moving along a path with one degree of freedom. The main characteristic of a ruled surface is that there is at least one straight line passing through the point of surface and lying entirely in the surface. In addition, every developable surface is a ruled surface [15]. As a result, modeling based on ruled surface is frequently used in constructing curved surfaces for aerospace industry and precision mechanical parts such as spatial cams, turbines, dies and molds, rotors of pumps, and centrifugal impellers. As the surface is normally twisted in design to achieve the required performance, collision and gouging problems have to be considered in specifying tool orientation for multi-axis machining.

The cutter location file of the ruled surface was generated by the sculptured method. Two popular milling approaches, the conventional point cutting method and the flank cutting technique can be adopted.

Compared with point cutting, flank milling can be efficiently applied to machine the ruled surface, which is performed by employing the side of a cutter to touch the desired ruled surface. Tsay and Her [11] developed a procedure for the five-axis flank milling of twisted ruled surface. An impeller with ruled blade surface was machined by the proposed technique using a five-axis machine tool with a cylindrical cutter. Young and Chuang [14] established an integrated five-axis machining module for a centrifugal impeller by combined related machining technologies. Leu et al. [7] described the sweep-envelope differential equation (SEDE) method and adopted it to compute the boundary points of the swept volumes generated by NC tools. Lartigue et al. [4] derived the envelope surface relying on kinematics parameters of the tool movement. The approach was applied on the particular case of flank milling of non-developable ruled surfaces.

The common machining method of the envelope surfaces is using a cutter of equal dimension to the meshing element. In this so-called “generating method”, the cutting tool followed the same path as the meshing element relative to the cam. The contact condition between

the form-mill cutter and surface was the line contact. In the manufacture for enveloping surfaces, Ivanov et al. [2] proposed a mathematical model for the determination of the profile of the helical surface when the tool geometry used and the parameters (machine setup) determining the tool orientation towards the blank were specified. Yan and Liu [13] and Lee and co-workers [6] integrated the activities for design and manufacturing of the variable pitch lead screw and roller gear cam. The interface between the CAM systems and NC machine tools is called the postprocessor. It converts cutter location file to NC code. In the research and development for postprocessor of machine tools, Sakamoto and Inasaki [10] classified the configuration of five-axis machine tools into three types. Warkentin et al. [12] presented a five-axis technique for machining of spherical surfaces with a radiused or flat bottom end mill. The NC data was generated for the wrist type five-axis machine tool. Lin and Lee [8] used the Denavit-Hartenberg (D-H) notation to produce and to measure the dimension accuracy of roller gear cams on 5-axis machine tools. Lee and She [5] developed a postprocessor for three kinds of five-axis machine tools. The analytical equations for NC data were obtained using the homogeneous coordinate transformation and inverse kinematics. Jung et al. [3] presented the algorithms for NC post-processing for typical five-axis milling machine of table-rotating/tilting type.

This paper describes the multi-axis toolpath generation using the flank milling method for the helical rotor. According to the geometry of the helical rotor, the cutter location file can be generated with a cylindrical end mill. The generated toolpath is converted to the analytical NC code expression by the postprocessor, taking account of the kinematic description of the multi-axis machine tool. To validate the NC program, a cutting simulation software, VERICUT®, is used to simulate the cutting geometry and kinematics. The trial cut is also performed with model material and demonstrates the practical application. Fig. 1 shows the flowchart of NC code generation for multi-axis machining of a helical rotor.

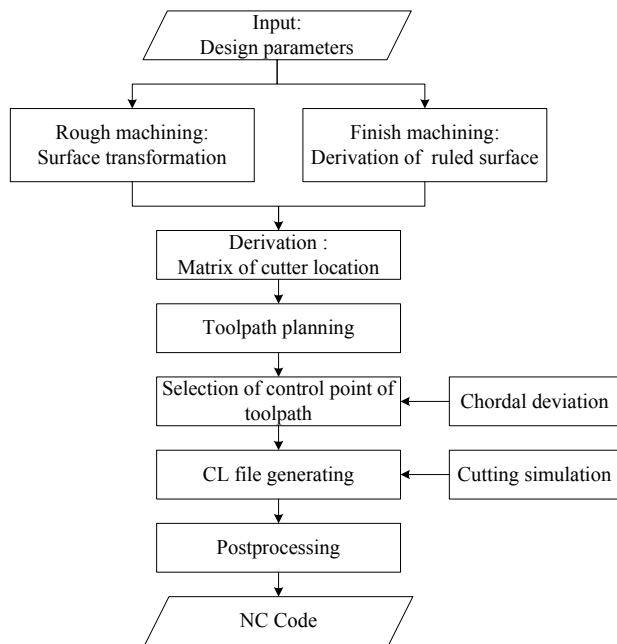


Fig. 1. Flowchart of multi-axis machining for helical rotor

## 2. Surface generation of helical rotor

### 2.1. Ruled surface

A ruled surface is generated by joining corresponding points on two space curves (directries) by straight lines, as shown in Fig. 2. A ruled surface is obtained by linearly interpolating between two known boundary curves associated with the opposite sides of the unit square in parametric space,  $P(0, \theta)$  and  $P(1, \theta)$ . The surface is given by

$$P(t, \theta) = P(0, \theta) + tu(\theta), \quad u(\theta) = P(1, \theta) - P(0, \theta) \quad (1)$$

$$0 \leq t \leq 1, \quad \theta_i \leq \theta \leq \theta_f$$

where  $P(0, \theta)$  and  $P(1, \theta)$  are named directries,  $u(\theta)$  is a ruling vector, and  $t$  is the parameter along the ruling. The corners of the surface are coincident with the ends of the given curve, and the appropriate edges of the blended surface are coincident with the given boundary curves.

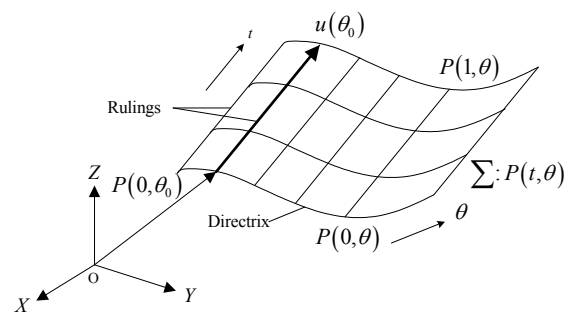


Fig. 2. Parametric representation of a ruled surface

### 2.2. Surface geometry of helical rotor

The geometry of the helical rotor is designed with variable pitch lead threads and variable groove depth, as shown in Fig. 3. Along the axial direction, the rotor is divided into ten regions from the inlet to exit. The helix angle is a constant in each region. The variable pitch lead threads and ditches are all ruled surface. In Fig. 3, a solid model built by Unigraphics NX is generated by the geometric parameters. The front view and the right view are shown in this figure. The directrix for a thread in the workpiece coordinate system (OXYZ)<sub>1</sub> is described as:

$$P(0, \theta) = \begin{bmatrix} r_h \cos \theta \\ r_h \sin \theta \\ -z_{o,n} - \tan \alpha_n r_h (\theta - \theta_{o,n} - \bar{\theta}) \\ 1 \end{bmatrix}, \quad \theta_{o,n} + \bar{\theta} \leq \theta \leq \theta_{1,n} + \bar{\theta} \quad (2)$$

This directrix is a helical curve on the thread tip. Where  $\bar{\theta}$  is the beginning revolution angle of a thread. The subscript  $n$  indicates the

$n$ th region,  $r_h$  is the outer diameter,  $\alpha$  is the helix angle of thread, and  $\theta$  is a parameter of rotating angle. In  $n$ th region, a rotor thread is from  $Z_{0,n}$  to  $Z_{1,n}$  in axial direction and rotation from  $\theta_{0,n}$  to  $\theta_{1,n}$  about axial direction.

The ditch is constructed by cone surface. The cone surface  $R(r,z)$  in  $n$ th region is described as:

$$R(\theta, z) = \begin{bmatrix} r(z) \cos \theta \\ r(z) \sin \theta \\ -z \\ 1 \end{bmatrix} \tag{3}$$

$$r(z) = r_{o,n} + \frac{z - z_{o,n}}{z_{1,n} - z_{o,n}} (r_{1,n} - r_{o,n}) \tag{4}$$

Based on the geometry of ditch, the directrix on the ditch surface can be expressed as:

$$P(1, \theta) = \begin{bmatrix} r(z) \cos \theta \\ r(z) \sin \theta \\ -z_{o,n} - \tan \alpha_n r_h (\theta - \theta_{o,n} - \bar{\theta}) \\ 1 \end{bmatrix} \tag{5}$$

The surface equation of the helical rotor and the unit normal vector are presented as follows:

$$P_1(t, \theta) = P_1(0, \theta) + t [P_1(0, \theta) - P_1(1, \theta)] \tag{6}$$

$$n_1(\theta) = \frac{\partial P_\theta(t, \theta) \times \partial P_t(t, \theta)}{|\partial P_\theta(t, \theta) \times \partial P_t(t, \theta)|} = \begin{bmatrix} -\sin \alpha_n \sin \theta \\ \sin \alpha_n \cos \theta \\ \cos \alpha_n \\ 0 \end{bmatrix} \tag{7}$$

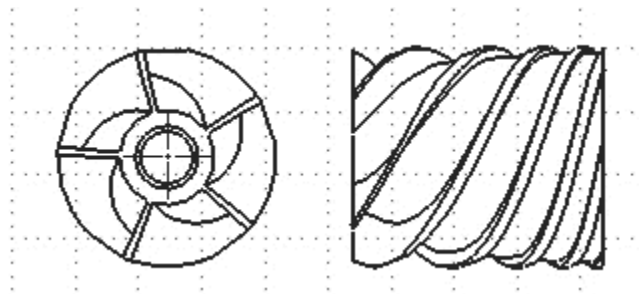


Fig. 3. Geometry of a helical rotor

### 3. Cutter location for machining helical rotor

In order to machine the ruled surface of the helical rotor, the orientation of the tool axis and the position of the cutter tip should be derived with respect to the workpiece coordinate system. To locate a cutter tangent to the ruled surface at the cutter contact point (cc), the cutter orientation is defined according to the unit ruling vector of the helical rotor. The unit ruling vector can be described as follows:

$$U_1(\theta) = \frac{u_1(\theta)}{|u_1(\theta)|} = [\cos \theta \quad \sin \theta \quad 0 \quad 0]^T \tag{8}$$

To obtain the position of the cutter tip, the cutter compensation vector ( $V$ ) is derived firstly. As shown in Fig. 4, the equation of compensation vector is

$$T = n_1 - (n_1 \cdot T_a) T_a \tag{9}$$

$$V = \frac{T}{|T|} \tag{10}$$

The tool position is determined by the Eq. 11

$$Q = P(t, \theta) + r_c \cdot V \tag{11}$$

where  $r_c$  is the cutter radius, and  $T_a$  is the tool axis,  $Q$  is the tool position.

The cutter location matrix with respect to the coordinate system  $(XYZ)_1$  of helical rotor can be expressed as follows:

$${}^1A_t = \begin{bmatrix} ? & ? & K_{x1} & Q_{x1} \\ ? & ? & K_{y1} & Q_{y1} \\ ? & ? & K_{z1} & Q_{z1} \\ 0 & 0 & 0 & 1 \end{bmatrix} \tag{12}$$

where the designation  ${}^iA_j$  indicates that the coordinate transformation is performed from  $(OXYZ)_j$  to  $(OXYZ)_i$ , the suffix  $t$  denotes the coordinate system at the tool tip.  $K_x, K_y, K_z$  are the components of tool orientation, and  $Q_x, Q_y, Q_z$  are the components of tool position.

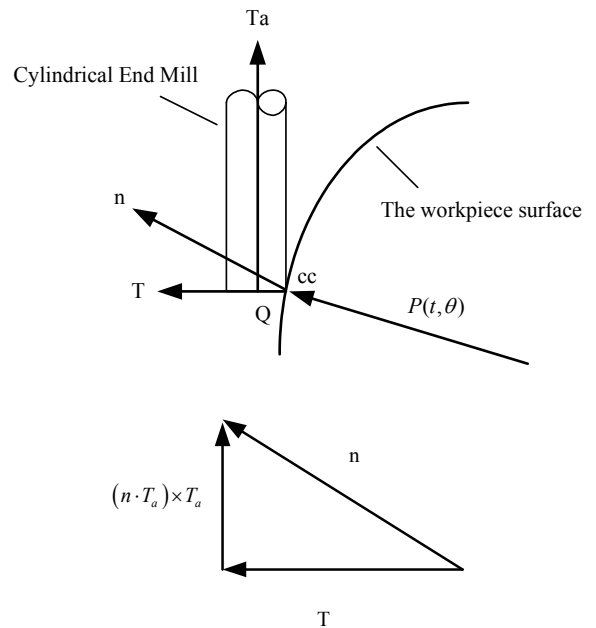


Fig. 4. Derivation of cutter position for cylindrical end mill

### 4. Analysis of chordal deviation

The chordal deviation ( $d_{n,n'}$ ) is shown in Fig. 5, can be expressed as follows (Faux and Pratt, 1979):

$$d_{n,n'} = (R_{n,n'} - R_n) - \frac{((R_{n,n'} - R_n) \cdot (T_n))T_n}{|T_n|^2} \quad (13)$$

where  $R_n$  is the position vector of the control point ( $P_n$ ),  $R_{n,n'}$  is the position vector of the checking point ( $P_{n,n'}$ ) and  $T_n$  is the chord vector determined from  $P_n$  to  $P_{n+1}$ .  $(( \cdot ) \cdot ( \cdot ))$  denotes the inner product. The design contour coincided with the manufacturing contour simultaneously is named the control point ( $P_n$ ).

The magnitude of chordal deviation,  $d_{n,n'}$ , can be calculated by taking the square root of the squared sums of the components of  $d_{n,n'}$  ( $d_{n,n'x}, d_{n,n'y}, d_{n,n'z}$ ):

$$d_{n,n'} = |d_{n,n'}| = (d_{n,n'x}^2 + d_{n,n'y}^2 + d_{n,n'z}^2)^{0.5} \quad (14)$$

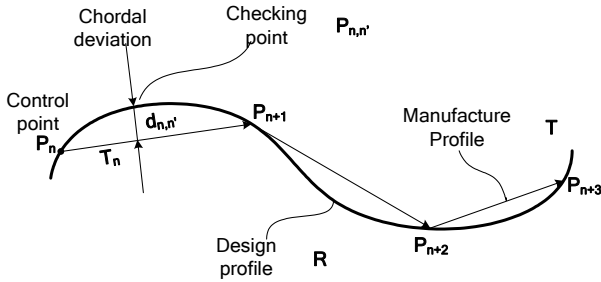


Fig. 5. Schematic illustration of chordal derivation

### 5. Postprocessor for table-tilting type five-axis machine tool

In order to establish the interface between the design and the manufacture of helical rotor, the postprocessor for multi-axis machine tool is developed. Once the cutter location file is obtained, it should be transformed into NC data using the inverse kinematics transformation for multi-axis machine tool. The inverse kinematics transformation depends on the structure of the multi-axis machine tool.

A table-tilting type five-axis machine tool is shown in Fig. 6. In addition to three linear perpendicular axes (X, Y, Z), the machine tool which has a rotary table C-axis and a tilting table (A-axis) rotating along the Z and X axes.

Referring to Fig. 7, coordinate systems  $(OXYZ)_w$  and  $(OXYZ)_i$  are defined at the workpiece and the cutting tool, respectively. The pivot points are located on the A axis and C axis. As shown in

Fig. 7, the pivot point  $R_A$  is the intersection of the two rotary axes, and the pivot point  $R_C$  is located on the rotational centre of C axis. The offset vector  $(L_{PSx}, L_{PSy}, L_{PSz})$  is constructed between the centers of the two rotary axes. The offset vector  $L_x i_w + L_y j_w + L_z k_w$  as determined from origin  $O_w$  to point  $R_C$  is required for the coordinate transformation. Since the structural elements of the machine tool consist of a rotary table, a tilting table, linear tables, machine bed, and cutting tool, the generating motion of the machine tool can be characterized sequentially from the workpiece to the cutting tool. It is referred to as the form-shaping function (Reshetov and Portman, 1988). By applying the homogeneous coordinate transformation matrix, the cutter location of the coordinate system  $(OXYZ)_i$ , with respect to workpiece coordinate system  $(OXYZ)_w$  is as follows:

$${}^w A_i = \begin{bmatrix} ? & ? & S\phi_z S\phi_x & \bar{Q}_x \\ ? & ? & C\phi_z S\phi_x & \bar{Q}_y \\ ? & ? & C\phi_x & \bar{Q}_z \\ ? & ? & 0 & 1 \end{bmatrix} \quad (15)$$

$$\bar{Q}_x = P_x C\phi_z + P_y S\phi_z C\phi_x + P_z S\phi_z S\phi_x + L_{PSx} C\phi_z + L_{PSy} S\phi_z + L_x \quad (16)$$

$$\bar{Q}_y = -P_x S\phi_z + P_y C\phi_z C\phi_x + P_z C\phi_z S\phi_x - L_{PSx} S\phi_z + L_{PSy} C\phi_z + L_y \quad (17)$$

$$\bar{Q}_z = -P_y S\phi_x + P_z C\phi_x + L_{PSz} + L_z \quad (18)$$

Eq. 15 describes the kinematic characteristics of the cutting tool mounted on the five-axis machine tool. ‘‘C’’ and ‘‘S’’ refer to the cosine and sine functions, respectively. The general form of the known cutter location matrix ( ${}^w A_i$ ) can be expressed as follows:

$${}^w A_i = \begin{bmatrix} ? & ? & K_x & Q_x \\ ? & ? & K_y & Q_y \\ ? & ? & K_z & Q_z \\ 0 & 0 & 0 & 1 \end{bmatrix} \quad (19)$$

By equating the corresponding elements of the third and fourth columns of Eq. 15 and Eq. 19, the rotation angles ( $\phi_A, \phi_C$ ) and the relative translation distances ( $P_x, P_y, P_z$ ) can be solved.

Since the program coordinate system is coincident with the workpiece coordinate system, it yields the following conditions:  $\phi_A = \phi_C = 0$  and  $[Q_{x0} Q_{y0} Q_{z0} 1]^T = [0001]^T$ . By equating the corresponding elements of the fourth column of Eq. 15, the relative translation distances ( $P_{x0}, P_{y0}, P_{z0}$ ) can be obtained.

$$\begin{bmatrix} P_{x0} \\ P_{y0} \\ P_{z0} \\ 1 \end{bmatrix} = \begin{bmatrix} -L_x - L_{PSx} \\ -L_y - L_{PSy} \\ -L_z - L_{PSz} \\ 1 \end{bmatrix} \quad (20)$$

The X, Y, Z values of the NC data can be presented as:

$$[X \ Y \ Z \ 1]^T = [P_x - P_{x0} \ P_y - P_{y0} \ P_z - P_{z0} \ 1]^T \quad (21)$$

Thus, the equations for NC data of this configuration can be expressed as follows:

$$A = \phi_x = a \cos(K_z), \quad 0 \leq \phi_x \leq \pi \quad (22)$$

$$C = \phi_z = a \tan 2(K_x, K_y), \quad -\pi \leq \phi_z \leq \pi \quad (23)$$

$$X = (Q_x - L_x)C\phi_z - (Q_y - L_y)S\phi_z + L_x \quad (24)$$

$$Y = (Q_x - L_x)C\phi_x S\phi_z + (Q_y - L_y)C\phi_x C\phi_z - (Q_z - L_z)S\phi_x - L_{p_{sy}}C\phi_x + L_{p_{sz}}S\phi_x + L_{p_{sy}} + L_y \quad (25)$$

$$Z = (Q_x - L_x)S\phi_x S\phi_z + (Q_y - L_y)S\phi_x C\phi_z + (Q_z - L_z)C\phi_x - L_{p_{sy}}S\phi_x - L_{p_{sz}}C\phi_x + L_{p_{sz}} + L_z \quad (26)$$

In the case of the tilting table, A is set to be 90°, only one rotation axis on the rotary table. This configuration of the five-axis machine tool is degenerated into four-axis machine tool. The analytical equations for NC data can be derived using the coordinate transformation matrices:

$$C = \phi_c = a \tan 2(K_x, K_z), \quad -\pi \leq \phi_c \leq \pi \quad (27)$$

$$X = (Q_x - L_x)C\phi_c - (Q_z - L_z)S\phi_c + L_x \quad (28)$$

$$Y = Q_y \quad (29)$$

$$Z = (Q_x - L_x)S\phi_c + (Q_z - L_z)C\phi_c + L_z \quad (30)$$

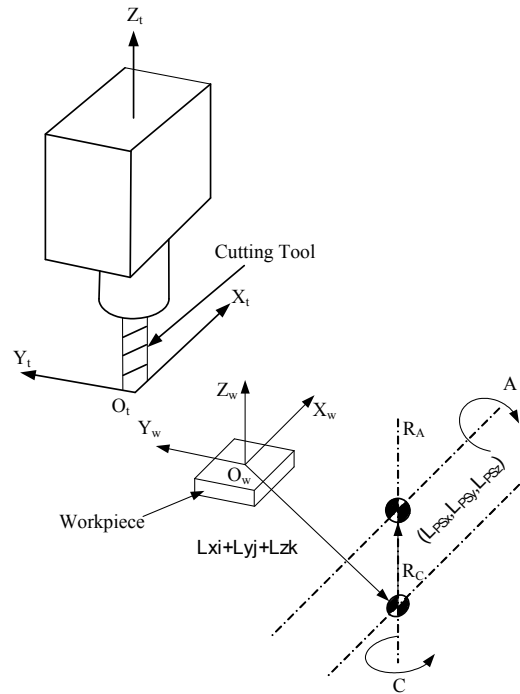


Fig. 7. coordinate systems of table-tilting type configuration

## 6. Implementation and verification

### 6.1. Design parameters and surface geometry of helical rotor

The design parameters of a variable pitch lead rotor as shown in Table 1, is used to verify the validity and effectiveness of the proposed methods. By substituting these parameters into Eqs. 2~7, the surface geometry of the helical rotor is obtained, as shown in Fig. 8. Fig. 8 (a) shows the directrices of ruled surfaces. Fig. 8(b) shows the cross-section profile of ditch surface. The solid model of a helical rotor built by CAD/CAM software is shown in Fig. 8(c).

Table 1. Design parameters of the helical rotor

| Region     | 1st   | 2nd     | 3rd   | 4th   | 5th   | 6th   | 7th   | 8th   | 9th   | 10th  |
|------------|-------|---------|-------|-------|-------|-------|-------|-------|-------|-------|
| O.D        | 103.4 | 103.4   | 103.4 | 103.4 | 103.4 | 103.4 | 103.4 | 103.4 | 103.4 | 103.4 |
| I.D        | 45    | 69.7    | 88.4  | 90.9  | 92.9  | 93.9  | 95.9  | 97.4  | 98.4  | 99.4  |
| $\alpha_n$ | 30    | 30      | 30    | 27.5  | 25    | 22.5  | 20    | 17.5  | 15    | 12.5  |
| $t_n$      | 3.0   | 3.0~5.6 | 5.6   | 5.6   | 5.6   | 5.6   | 5.6   | 5.6   | 5.6   | 5.6   |
| $z_n$      | 22.5  | 17.5    | 10    | 10    | 10    | 10    | 10    | 10    | 10    | 10    |
| $\theta_n$ | 43.0  | 33.5    | 19.5  | 21.0  | 23.5  | 27.0  | 30.5  | 35.0  | 41.0  | 50.0  |

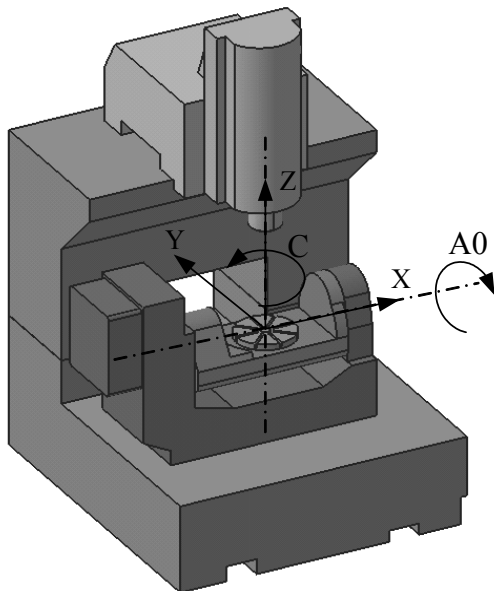


Fig. 6. Configuration for table-tilting type five-axis machine tool

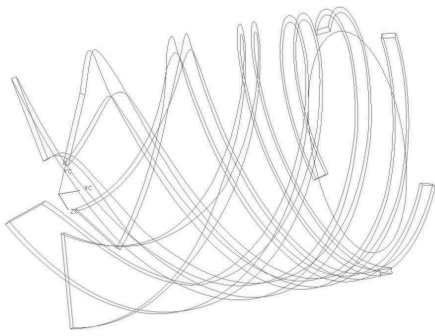


Fig. 8a. Solid model of a helical rotor built by Unigraphics NX. Directrices of a variable pitch lead rotor

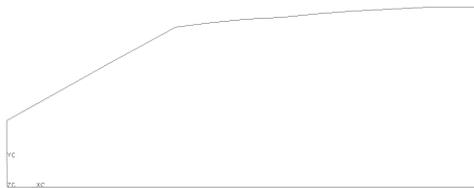


Fig. 8b. Solid model of a helical rotor built by Unigraphics NX. The cross-section profile of ditch surface

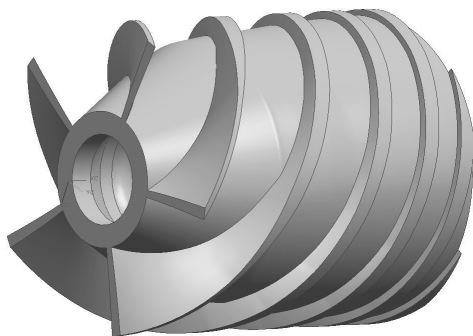


Fig. 8c. Solid model of a helical rotor built by Unigraphics NX. Surface geometry of a helical rotor

### 6.2. Toolpath generation

The concept used in selecting control points on the toolpath is to use the least control points and keep the surface mathematical error within the given tolerance. By means of the procedure of error control, the least control points on the toolpath and the appropriate path interval distance can be obtained by the numerical iteration method. Table 2 shows the used machining parameters corresponding to various machining process. Fig. 9 reveals the toolpath of four-axis machining for grove geometry and thread blade using cylindrical end mill.

Table 2. Machining parameters for helical rotor

| Machining Process     | Cutting Tool                  | Chordal Deviation | Cutting Method |
|-----------------------|-------------------------------|-------------------|----------------|
| Rough Machining       | $\phi 8$ Cylindrical End Mill | 0.1mm             | Zig-zag        |
| Semi-finish Machining | $\phi 8$ Cylindrical End Mill | 0.05mm            | Zig            |
| Finish Machining      | $\phi 8$ Cylindrical End Mill | 0.01mm            | Zig            |

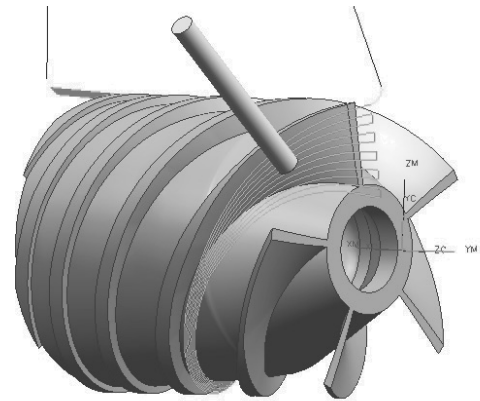


Fig. 9a. Toolpath generation of four-axis machining for helical rotor. Toolpath of rough machining for groove geometry

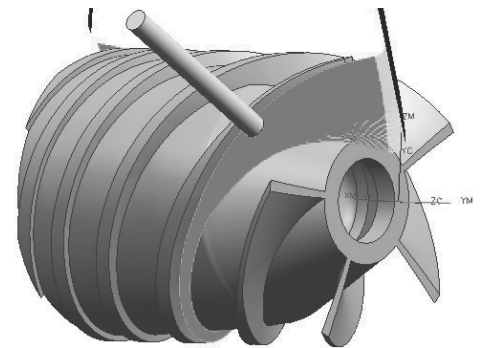


Fig. 9b. Toolpath generation of four-axis machining for helical rotor. Toolpath of finish machining for thread blade

### 6.3. Toolpath simulation

To avoid the risk of human error, the generated toolpath should be verified before actual machining. Fig. 10(a) presents the process of rough machining by the proposed method with cylindrical end mill simulated by VERICUT<sup>®</sup> software. Fig. 10(b) shows the process of finish machining. The simulation results demonstrate that the machining process works well and the collision between the shank and workpiece surface does not

occur. After the simulation and the verification, the generated toolpath is converted into NC program by the developed postprocessor. The five-axis machine tool is used to perform the actual machining. Fig. 11 shows the machining workpiece with rotor profile.



Fig. 10. The four-axis machining of model material on five-axis machine tool

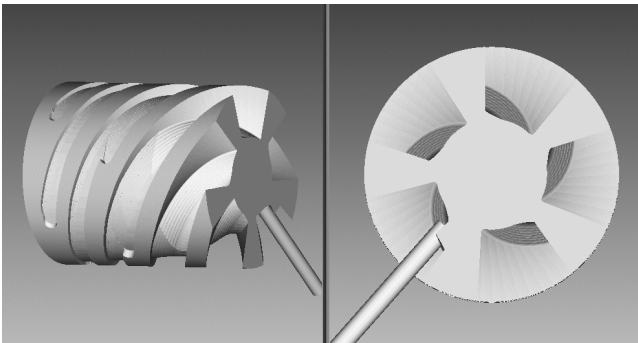


Fig. 11a. Rough machining for groove geometry (Tool diameter 8mm)

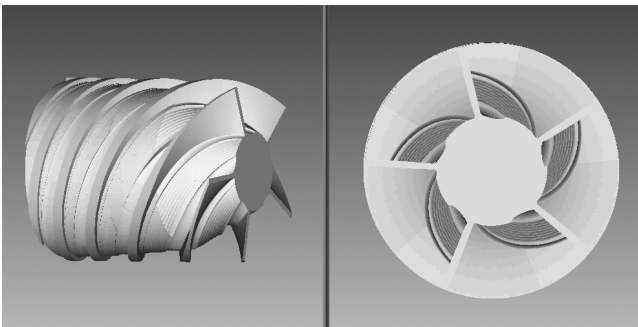


Fig. 11b. Finish machining for thread blade (Tool diameter 8mm)  
Figure 10: Simulation of helical rotor cutting by the proposed method

## 7. Conclusions

This paper presented a method for generating the toolpaths for the machining of a helical rotor on five-axis machine tool. The geometry of the helical rotor is designed based on the ruled surfaces. Through the homogeneous coordinate transformation, the cutter location of the flank milling for four-axis machining can be generated. The postprocessor are developed for converting the cutter location file to the four-axis numerical control program. The toolpath generated are verified through solid cutting simulation and a trial cut. The results show that the proposed method is valid and the machining process works well.

## Acknowledgements

The authors would like to thank the support of the National Science Council, Taiwan, R.O.C. under grant NSC 95-2622-E-230-008-CC3.

## References

- [1] I.D. Faux, M.J. Pratt, Computational Geometry for Design and Manufacture, Ellis Horwood, Chichester, U.K. 1979.
- [2] V. Ivanov, G. Nankov, V. Kirov, CAD Orientated Mathematical Model for Determination of Profile Helical Surfaces, International Journal of Machine Tools and Manufacture 38 (1998) 1001-1015.
- [3] Y.H. Jung, D.W. Lee, J.S. Kim, H.S. Mok, NC Post-processor for 5-axis Milling Machine of Table-rotating/tilting Type, Journal of Materials Processing Technology 130-131 (2002) 641-646.
- [4] C. Lartigue, E. Duc, A. Affouard, Tool Path Deformation in 5-axis Flank Milling Using Envelope Surface, Computer Aided Design 35 (2003) 375-382.
- [5] R.S. Lee, C.H. She, Developing a Postprocessor for Three Types of Five-axis Machine Tools, International Journal of Advanced Manufacturing Technology 13 (1997) 658-665.
- [6] R.S. Lee, J.N. Lee, A New Method of Tool Orientation Determination by Enveloping Element for 5-axis Machining of Spatial Cam, International Journal Production Research 40 (2002) 2379-2398.
- [7] M.C. Leu, L. Wang, D. Blackmore, A Verification Program for 5-axis NC Machining with General APT Tools, Annals of the CIRP 46 (1997) 419-424.
- [8] P.D. Lin, M.F. Lee, Applications of D-H Notation in Machining and On-line Measurement of Roller-gear Cams on 5-axis Machine Tools, Journal of Manufacturing Science and Engineering 119 (1997) 393-401.
- [9] D.N. Reshetov, V.T. Portman, Accuracy of machine tools, ASME, New York, 1988.
- [10] S. Sakamoto, I. Inasaki, Analysis of Generating Motion for Five-axis Machining Centers, Transactions of the Japan Society of Mechanical Engineers 59 (1993) 1553-1559.

- [11] D.M. Tsay, M.J. Her, Accurate 5-axis Machining of Twisted Ruled Surfaces, *Journal of Manufacturing Science and Engineering* 123 (2001) 731-738.
- [12] A. Warkentin, S. Bedi, F. Ismail, Five-axis Milling of Spherical Surfaces, *International Journal of Machine tools and Manufacture* 36 (1996) 229-243.
- [13] H.S. Yan, J.Y. Liu, Geometry Design and Machining of Variable Pitch Lead Screws with Cylindrical Meshing Elements, *Journal of Manufacturing Science and Engineering* 115 (1993) 490-495.
- [14] H.T. Young, L.C. Chuang, An Integrated Machining Approach for a Centrifugal Impeller, *International Journal of Advanced Manufacturing Technology* 21 (2003)556-563.
- [15] I. Zeid, *CAD/CAM Theory and Practice*, McGraw-Hill, Inc. 1991.